Bioresource Technology 365 (2022) 128161

Contents lists available at ScienceDirect

Bioresource Technology

journal homepage: www.elsevier.com/locate/biortech

Transition roadmap for thermophilic carbon dioxide microbial electrosynthesis: Testing with real exhaust gases and operational control for a scalable design

Laura Rovira-Alsina, M. Dolors Balaguer, Sebastià Puig *

LEQUiA. Institute of the Environment, University of Girona, Campus Montilivi. C/Maria Aurèlia Capmany, 69, E-17003 Girona, Catalonia, Spain

HIGHLIGHTS

- Thermophilic operation boosts selectivity and exploits waste heat from gas emissions.
- Real off-gases were tested and proved not to hamper productivity in the long term.
- A fully automated bench-scale system was designed, set-up and operated.
- 2 kg of CO_2 were reduced for every kg of acetate produced.
- Galvanostatic control allowed low energy consumption (2 kWh per kg of acetate)

GRAPHICAL ABSTRACT

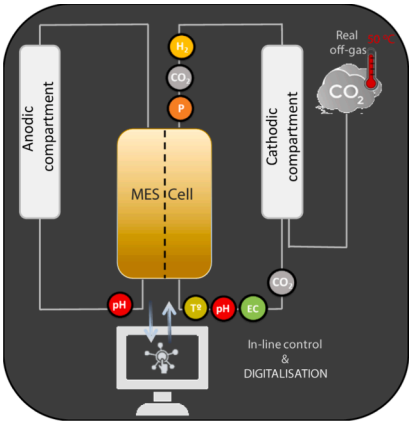

ARTICLE INFO

Keywords:
Acetate production
Carbon conversion
Flue gas
Galvanostatic control
Power to Product ratio

ABSTRACT

Human activities release more carbon dioxide (CO_2) into the atmosphere than the natural process can remove. This study attempts to address the main challenges for the thermophilic (50 °C) bioelectrochemical conversion of CO_2 into acetate. First, real gaseous emissions were tested with mixed microbial consortia, which had no substantial influence on production rates (difference of 2.5%). Subsequently, a bench-scale system (TRL 4–5) was designed and launched to control key operational variables. Fixing the current at 1.3 A m^{-2}, CO_2 was reduced at a rate of 2.21 kg CO_2 kg^{-1} acetate, while the electricity consumption was 2.07 kWh kg^{-1}, the most efficient value so far. The results suggest that the operation with real effluents is feasible and the proposed design is energy efficient, but the right balance between maximising current densities without compromising the biocompatibility with catalysts will determine the transition from laboratory scale towards its implementation in the market.

* Corresponding author.
E-mail address: sebastia.puig@udg.edu (S. Puig).

https://doi.org/10.1016/j.biortech.2022.128161
Received 9 September 2022; Received in revised form 13 October 2022; Accepted 14 October 2022
Available online 19 October 2022

1. Introduction

The severity of the anthropogenically induced climate change depends not only on the magnitude of the change, but also on the potential for irreversibility. The impact resulting from the increased carbon dioxide (CO_2) concentration is largely irreversible for 1000 years after emissions cease (Solomon et al., 2009). Nevertheless, microbial electrosynthesis (MES) of organic compounds from CO_2 is a potential alternative for capturing and storing this greenhouse gas in the long term (Bian et al., 2020). It allows the production of value-added compounds from harmful waste without the need to use scarce and environmentally unfriendly raw materials that can trigger conflicts between politically unstable countries (Bajracharya, 2016). However, this technology is still at low technology readiness levels (TRLs) (Virdis et al., 2022), and still needs multiple-steps to scale up and reach a competitive position in the market (Fruehauf et al., 2020). Many efforts have been devoted to deciphering the metabolic pathways responsible for the reduction of CO_2 to different compounds such as methane (Van Eertenjansen et al., 2012), ethanol (Romans-Casas et al., 2021), butyrate (Batlle-Vilanova et al., 2017), caproate (Jourdin et al., 2018), among others (Vassilev, 2019), depending on the microbial culture and operational conditions used. Nevertheless, the most ancient metabolism for CO_2 fixation is the Wood-Ljungdahl pathway, in which hydrogen (H_2) is used as an electron donor and CO_2 as an electron acceptor to obtain acetate (HA) (Schuchmann and Müller, 2014). This is a platform compound with lower economic value compared to others (Jourdin et al., 2020), but with a huge potential to be used as a precursor for different products such as plastics, dyes, inks, pesticides, rubbers, detergents and pharmaceuticals (Verbeeck, 2014). Today, the technology needs to get closer to industrial deployment moving out of the laboratory and start using affordable materials for the scale-up, treating gaseous effluents, and operating at conditions similar to where it could be implemented (Christodoulou et al., 2017). Even though most of the studies are carried out under mesophilic conditions, the possibility of operating these systems at higher temperatures (greater than50 °C) to exploit the residual heat from CO_2 point emissions (e.g. cement plants) has proven to be an effective approach to reduce microbial competition and thus, increase the selectivity of the final product (Rovira-Alsina et al., 2020). The different reactions that can occur depending on the biological catalyst used (Von Stockar et al., 2006) and the operational parameters (Angenent et al., 2016) have also been studied from a thermodynamic perspective. Again, granted a simple and scalable design for industrial application, the most thermodynamically favourable compound to be obtained in any of the usual combinations of variables is HA (Rovira-Alsina et al., 2022). On the other hand, given that these systems require an electrical input to drive the thermodynamically unfavourable reactions (Rabaey and Rozendal, 2010), their integration with renewables is the most viable option. Some studies rely on the transition of the public grid to increase the share of energy from renewables (Dessì et al., 2020), but the use of MES to store excess energy when it exceeds demand is also an attractive option to be considered (Rovira-Alsina et al., 2021; Su and Ajo-Franklin, 2019).

Therefore, studies using real off-gases are needed to assess how microbial consortia would adapt to an impure CO_2 effluent and how this would affect production rates and overall performance. In this sense, the transition to higher TRLs will require implementing a digital transformation to help monitor, control and operate in the most efficient, sustainable and competitive way the MES systems. The present study aimed at testing a real CO_2 stream for its thermophilic bioelectroconversion to HA and applying all the background knowledge to design and start up for the first time, a fully automated bench-scale system.

2. Materials and methods

2.1. Inoculum and growth media

The microbial community was taken from an anaerobic digester working at 37.5 °C of a wastewater treatment plant (WWTP) located in Girona, Spain. A 1:20 dilution with a synthetic solution based on ATCC1754 growth medium (Tanner et al., 1993) was incubated in 50 °C fermentative reactors under H_2:CO_2 (80:20 *v/v*) to promote acetogenesis and microorganisms' adaptation to thermophilic conditions. During this enrichment stage, pH was adjusted to 6 and 2-bromoethanesulfonic acid (10 mM) was added to prevent methanogenesis (Jadhav et al., 2018). Two additional 1:20 dilutions of this inoculum with the reformulated medium to remove all sources of organic carbon were performed before inoculating the reactors. All the experiments were carried out with the same adapted inoculum after an initial growth period of at least 30 days.

2.2. Batch tests with real off-gas supply. Set-up and operation

Two MES systems named HT1 and HT2 were constructed for real CO_2 testing. They consisted of two identical glass H-type bottles (Pyrex V-65231 Scharlab, Spain), separated by a cation exchange membrane of $2{\cdot}10^{-4}$ m^2 (CMI-1875 T, Membranes International, USA). The cathode consisted of a plain carbon cloth (thickness of 490 μm, working area of $3.0{\cdot}10^{-3}$ m^2 for HT1 and of $1.2{\cdot}10^{-3}$ m^2 for R2; NuVant's Elat LT2400 FuelCellsEtc, USA) connected to a stainless-steel wire. The anode was a $2{\cdot}10^{-6}$ m^3 graphite rod of 0.1 m in length and $5{\cdot}10^{-3}$ m in diameter (EnViro-cell, Germany). An Ag/AgCl electrode (+0.197 V *vs* SHE (standard hydrogen electrode), model rE-5B, BASI, UK) with an operating temperature range from 0 to 60 °C was placed in the cathodic chamber and used as a reference electrode. Reactors were sealed with butyl rubber caps to prevent gas leakage and keep the headspace volume of each chamber at 0.03 L (for HT1) and 0.01 L (for HT2), while the liquid volume accounted for 0.22 L in HT1 and 0.09 L in HT2. Both MES systems were operated in a three-electrode configuration with a potentiostat (BioLogic, Model VSP, France), which controlled the cathode potential at −0.8 V *vs* SHE and monitored the current density over time. All the potentials reported in this work are relative to SHE unless otherwise noted. Before use, the working electrodes were pre-treated in a 0.5 M solution of HCl and 0.5 M of NaOH for a total of two days and rinsed with deionized water for an additional day. At the end of the experimental study, the voltage of the reference electrodes was measured to ensure any shift that may have occurred during operation. The temperature was kept constant at 50 °C and an agitation rate of 80 rpm was fixed using a magnetic stirrer (Agimatic-ED-C; Scharlab, Spain) to enable mixing and facilitate mass transfer inside the cathodic chambers. All reactors were operated in batch mode and kept in the dark to avoid the growth of phototrophic microorganisms.

Either pure CO_2 (99.9%, Praxair, Spain) or real CO_2 off-gas coming from an industrial relevant gas emitter (main components: 74% nitrogen (N_2), 14% CO_2 and 12% oxygen (O_2)) was sparged for 10 min in the cathodic chamber twice a week to oversaturate the liquid media and renew the headspace. Additionally, it was added or removed punctually from 1 to 5 times per week to ensure a gas pressure between 1 and 2 atm. Samples from the liquid phase were taken before bubbling and the withdrawn liquid was replaced with a freshly prepared medium to maintain constant volumes in both chambers. The initial pH was set at 6, and it was modified with a basic solution (NaOH 1 M) when required. Electric conductivity (EC) and pH were measured with an electrical conductivity meter (EC-meter basic 30+, Crison, Spain) and a multimeter (MultiMeter 44, Crison, Spain), respectively. The optical density (OD) of the bulk liquid was also measured to control the growth of the planktonic microbial community with a spectrophotometer (Thermo Fisher Scientific, USA) at a wavelength of 600 nm. Gas pressure in the headspace of the reactors was measured using a digital pressure sensor (differential pressure gauge, Testo 512, Spain).

2.3. Bench-scale system: Instrumentalisation, set-up and operation

A fully equipped bench-scale bioelectrochemical system was designed and set up for dynamic control of the operational variables using pure CO_2 (99.9%, Praxair, Spain) as feed. The pH (easySense pH 32; Mettler Toledo, Spain), EC (easySense Cond 77; Mettler Toledo, Spain), pressure (PA3526; ifm, Spain), temperature and dissolved CO_2 (InPro® 5000(i); Mettler Toledo, Spain), H_2 (H2100 microsensor; Unisense, Denmark) and O_2 (easySense O_2 21; Mettler Toledo, Spain) content were monitored by in-line probes in the recirculation loop using a continuous stirred probe holder (HYCC, EEUU) (see supplementary material). They were controlled by actuator pumps and a multi-transmitter (Multi-parameter Transmitter M200; Mettler Toledo, Spain) that supplied the required component on demand through a remote access tool (EasyAccess 2.0) and an operation interface software (cMT Viewer). An Ag/AgCl reference electrode was placed also in the recirculation loop for proper electrochemical control. Liquid CO_2 concentration was kept between a maximum range from 600 to 1200 mg L^{-1} by using a magneto-inductive flowmeter (SM4100; ifm, Spain) installed and connected to a gas bottle (99.9% CO_2) to keep the set point. An ON/OFF pH control system pumped HCl or NaOH 5 M solutions using electromagnetic diaphragm dosing pumps (DOSATec PCO; Dosatronic, Spain) to the medium when required, maintaining a pH range between 4.5 and 7. Gas flow meters (Digital Flow Switch PF2M721; SMC, Spain) were installed in the inlet and outlet of the circuit to quantify the CO_2 conversion and H_2 production rates. The bench-scale installation was assessed with two different reactor configurations, though all were operated in batch mode and kept in the dark to avoid the growth of phototrophic microorganisms.

Two Electro MP Cells (ECell model 1735; ElectroCell A/S, Denmark) were constructed consisting of two stainless steel end plates, compacting two types of electrolyte distributor racks (PVDF frame sets) that separated up to two anodic compartments from three cathodic ones by cationic exchange membranes (Nafion N324) (see supplementary material). 1 mm EPDM rubber gaskets were placed between the PVDF frame sets to avoid leaks. The electrodes consisted of graphite plates (SIGRAFINE® R8710; FuelCellStore). Three of them could function as working electrodes (4 operative faces; working area of 0.04 m^2) and the two rest could serve as counter electrodes (4 operative faces; working area of 0.04 m^2). The ECells were operated under galvanostatic control through a programmable logic controller (Haiwell PLC - H02PW, China) connected to a power supply unit (MQR120-24F; Mibbo, China), fixing the cathodic current and tracking the cell voltage evolution over time. The cathodic and anodic compartments of the ECell accounted for 0.4 L each, and the medium was injected in parallel from the bottom to the top of the cell, following a cross-flow. Each compartment was connected to an external circuit with additional vessels and probe holders, increasing the volume of the cathodic circuit to 3.5 L and the anodic circuit to 2.5 L, keeping 0.1 L for the headspace. The current of the working electrode was fixed from 0.5 to 5 A m^{-2} and the temperature at 50 °C using a circulation ultra-thermostat (Digit-cool 3001373; Selecta, Spain) and a thermal heating mat (Lerway, Spain). Good mixing conditions were assured with a micro-pump (85376; MicroPump, USA) that recirculated the medium at a flow rate of 0.1 L min^{-1}.

A flat plate reactor (FP) was additionally constructed consisting of two methacrylate compartments of 0.185 L each separated by a cationic exchange membrane (CMI-1875 T, Membranes international, USA) of 0.008 m^2 (4.4 cm width and 18.8 cm length). The anode consisted of 0.013 m^2 (4.3 cm width and 15 cm length) of commercial carbon cloth (Thickness 490 μm; NuVant's ELAT, LT2400W, FuelCellsEtc, USA) connected to a carbon rod (0.45 cm diameter and 4.4 cm of length, Mersen Iberica, Spain) and the same, a 0.013 m^2 carbon cloth in contact to a carbon rod was used as a cathode electrode. The reactor was operated under galvanostatic control fixing the cathodic current at 5 A m^{-2} and the same temperature and mixing conditions as in the ECells were applied for this set-up.

To assess the performance of reactors, gas samples were daily taken to check and recalibrate the dissolved gas sensors, while liquid samples were taken from 2 to 7 days per week, depending on the experiment, for the quantification of volatile fatty acids. At the end of each test, 80% and 100% of the cathodic and anodic media, respectively, were drained and replaced with fresh medium to start the following one.

2.4. Analyses and calculations

The concentration of organic compounds (volatile fatty acids and alcohols) in the liquid phase was determined using an Agilent 7890A gas chromatograph equipped with a DB-FFAP column and a flame ionization detector. Production rates of HA (g L^{-1} d^{-1} or g m^{-2} d^{-1}) were calculated considering the total cathodic volume (0.22 and 3.50 L for the HT and bench-scale systems, respectively) or the total surface of the cathode (0.003 and 0.040 m^2, respectively). Gas samples were analysed by gas chromatography (490 Micro GC system, Agilent Technologies, US) equipped with two columns: a CP-molesive 5A for methane (CH_4), carbon monoxide (CO), H_2, O_2 and N_2 analysis, and a CP-Poraplot U for CO_2 analysis. The two columns were connected to a thermal conductivity detector (TCD).

In HT reactors, the concentrations of dissolved H_2, CO_2 and O_2 in the liquid media were calculated using Henry's law at 50 °C (Equation (1)), where C_i is the solubility of a gas in a particular solvent (mol L^{-1}), H_i is the Henry's law constant in mol L^{-1} atm^{-1} (0.0007 for H_2, 0.0195 for CO_2 and 0.0009 for O_2) and $P_{gas\,i}$ is the partial pressure of the gas in atm.

$$C_i = H_i\, P_{gas\,i} \tag{1}$$

The coulombic efficiency (CE) for the conversion of the current into products (i.e. H_2, HA, O_2) was calculated according to Patil et al. (2015) (Equation (2)), where C_i is the compound i concentration in the liquid phase (mol C_i L^{-1}), n_i is the molar conversion factor (2, 8 and 4 $moleq^{-1}$ for H_2, HA and O_2, respectively), F is the Faraday's constant (96485C mol e^{-1}), $VNCC$ is the net liquid volume of the cathode compartment (L), and I the current density of the system (A).

$$CE(\%) = \frac{C_i \sum_i n_i F V_{NCC}}{\int_0^t I dt} \tag{2}$$

3. Results and discussion

3.1. Microbial electrosynthesis of acetate using real off-gases

Two HT reactors were operated during a 100-days experimental period. Both HTs behaved similarly in terms of gas composition and HA production, although HT2 had lower production rates, probably related to the smaller surface area of the cathode electrode (Patil et al., 2015). They were fed with synthetic gas (100% CO_2) twice a week from day 0 to day 53, and then replaced with real off-gas (14% CO_2 and 12% O_2) for the rest of the trial (Fig. 1). HA was produced from day 1, maintaining similar rates until day 28, which caused a decrease in pH from 6.4 to 4.5, when its concentration stopped increasing due to nutrient limitation (Rovira-Alsina et al., 2020). OD also dropped, probably because the cells adhered to the electrode until HA production ceased, leading to an accumulation of H_2 in the headspace which elevated the gas pressure, pH and also OD. On day 42, a new batch was started by exchanging part of the liquid for fresh medium, which further increased the pH and decreased the OD. HA production was restarted and the change of gas supply (from synthetic to real gas) did not seem to affect its production, which remained at a similar slope (81 *vs* 79 mg L^{-1} d^{-1}) until day 75, before a new batch was performed. During this period, the percentage of CO_2 in the headspace decreased an 86% while O_2 was a 12% higher than before, balancing the ratios between the two gases, while some of the H_2 produced accumulated again in the gas phase together with N_2, that not being used, was the most abundant compound (around 80%). As the HA concentration increased, the pH decreased again and, interestingly, the

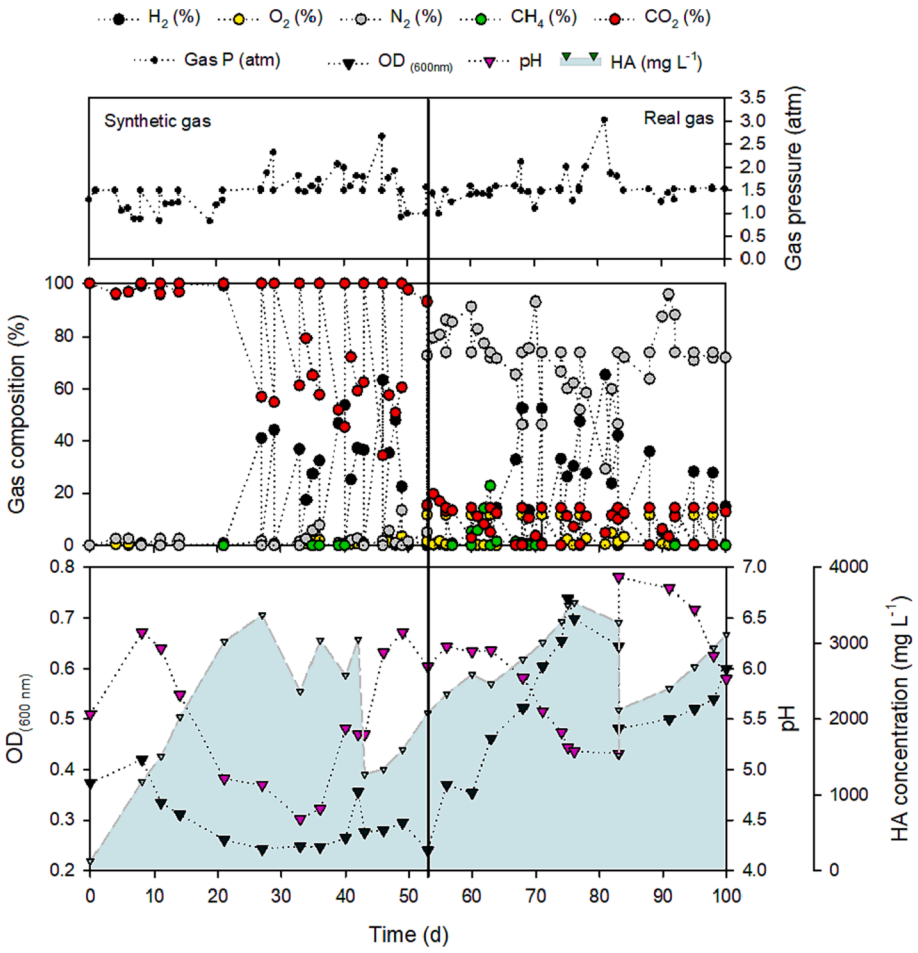

Fig. 1. Variation of the gas and liquid phases of the HT1 reactor over time under a cathodic potential of −0.8 V *vs* SHE. OD: Optical Density at 600 nm; HA: Acetate. The vertical black line separates the period of synthetic CO_2 feed from the period with real off-gas addition.

OD rose from 0.2 to 0.7 units due to the eventual development of a mixed microbial community with O_2 scavengers, acetogens and methanogens that when pH was above 6, produced up to 23% of CH_4. The latter could be inhibited by a single addition of 1 g L^{-1} of 2-bromoethanesulfonic acid.

A more detailed analysis of specific production periods (Table 1) showed that during the synthetic gas feed, all the CO_2 supplied and H_2 produced were devoted to HA production, reaching a CE_{HA} between 80 and 100%. At a fixed cathode potential of −0.8 V, the current density remained constant at 1.8 A m^{-2} and OD values decreased. Even though the maximum HA production rate (10.4 g m^{-2} d^{-1}) was obtained during the first period after inoculation (from day 0 to 28), the switch to real gas feeding did not change the production slope, which in that period (from day 42 to 53) was about 6 g m^{-2} d^{-1}. However, the composition of the gas varied, reducing the CO_2 partial pressure from 1.2 to 0.5 atm and, conversely, increasing the O_2 partial pressure to 0.4 atm. The change in the gas feeding decreased the current density until, after a period of adjustment, it gradually started to increase, reaching up to 0.5 A m^{-2} more than before, but the direction of the electrons was split, giving a CE_{HA} of 45% and a CE_{H2} of 25%, while only some of the electrons were used for O_2 reduction (<3%). Yet, HA production yielded a higher rate (8.4 g m^{-2} d^{-1}) and OD increased, suggesting that most of the O_2 was consumed by microorganisms in the bulk liquid rather than being electrochemically reduced.

Table 1
Acetate (HA) production rate (g m^{-2} d^{-1}), optical density (OD_{600nm}) variation (u d^{-1}), gases (CO_2 and O_2) partial pressures (atm), coulombic efficiencies (CE % of HA, H_2 and total) and average current density (A m^{-2}) of HT1 during production periods using synthetic (from day 41 to 53) and real off-gas feed (from day 53 to 75). The cathodic potential was fixed at −0.8 V *vs* SHE.

	Synthetic gas	Real off-gas
HA production rate (g m^{-2} d^{-1})	5.94 ± 1.78	5.79 ± 0.12
OD_{600nm} (u d^{-1})	−0.012 ± 0.010	0.023 ± 0.010
P_{CO2} (atm)	1.2 ± 0.3	0.5 ± 0.2
P_{O2} (atm)	0.01 ± 0.01	0.40 ± 0.20
CE_{HA} (%)	90 ± 10	45 ± 5
CE_{H2} (%)	5 ± 2	25 ± 5
CE_{tot} (%)	95 ± 5	73 ± 6
Current density (A m^{-2})	1.8 ± 0.1	2.3 ± 0.3

The presence of O_2 in the real off-gas (12%) was expected to have an impact either by increasing the current density for O_2 reduction or by decreasing HA production. Despite, the results showed that the use of untreated gas was not detrimental to the microbial community nor HA production. Taking into account the stoichiometric HA formation from H_2 and CO_2 and its oxidation back to CO_2 and H_2O under the applied conditions, the saturation with real exhaust gas implied a theoretical 85% reduction in HA production. However, during the period of synthetic CO_2 use, the systems were overfed, always retaining residual CO_2 in the headspace (around 50%). Although the presence of O_2 increased the power consumption by 28% and decreased the CE by 23% (Table 1), the microbial optical density increased sufficiently to maintain anaerobic conditions and similar production rates.

After saturation, O_2 was normally depleted within one day, while CO_2 was consumed progressively over three days, until it was completely exhausted. If a minimum of CO_2 could have been maintained

in the system through a more frequent gas supply, production rates would probably have been higher. The maximum HA production rates (10.4 and 8.4 g m^{-2} d^{-1} for synthetic and real CO_2, respectively) and the CE obtained (100% and 79%) are among the results of most MES studies reported so far with similar carbon materials and fixed potentials (Mateos et al., 2019; Song et al., 2019; Yang et al., 2021). So far, this is the first study operating with real gases and thermophilic conditions for more than 1 month, and these reactors continue running and producing at similar rates. The only study that also used industrial CO_2 for acetate production *via* MES (Roy et al., 2021) obtained lower cumulative HA concentration (1.8 g L^{-1}) but a higher production rate (65 g m^{-2} d^{-1}). However, the used off-gas was obtained from a brewery industry containing mainly CO_2 (97.9% of CO_2, 1.7% of N_2 and 0.4% of O_2), being much purer compared to the off-gas tested in the present study.

3.2. Galvanostatic control adjustment for efficient energy use

Previous tests under similar conditions (50 °C, open culture, carbon-based electrodes and CO_2 feed; Rovira-Alsina et al., 2020; Rovira-Alsina et al., 2021) had been carried out by fixing the cathodic potential. The potentiostatic control may be useful in narrowing down the electron transfer mechanisms possibly involved and may lead to the formation of a more energy-efficient microbial community. However, when thinking about scaling up the technology, constant current (galvanostatic control) may allow better control of production rates and selectivity, as it is less sensitive to local changes (e.g. pH) and the electron flow can be controlled to stoichiometrically match the CO_2 supply rate (Molenaar et al., 2017).

The ECells were inoculated and operated for 15 days to start up the reactor and condition the microbial biomass to the new configuration. Several short tests were consecutively performed at different fixed intensities ranging from 0.5 to 5.0 A m^{-2} (Fig. 2). At 0.5 A m^{-2}, there was almost no HA production and the low power consumption accounted for H_2 production. At 1.0 A m^{-2}, part of the CO_2 was consumed for HA generation, but the increased electrical input was not proportional compared to the amount required at 1.3 A m^{-2} for the improved HA production rate (1.23 *vs* 5.59 g m^{-2} d^{-1}) (Table 2). Subsequently, the current supply was cut off and the remaining H_2 was almost entirely consumed to produce more HA, albeit at a slower rate (1.39 g m^{-2} d^{-1}). At this point, a new batch was started at 1.5 A m^{-2} in which a lower HA production rate was obtained (4.25 g m^{-2} d^{-1}) compared to at 1.3 A m^{-2} while more unused H_2 accumulated in the medium. Increasing the current to 5.0 A m^{-2} resulted in a significant change in power consumption (an order of magnitude (Wh d^{-1}) higher compared to any other condition), but this was not followed by a higher HA production, rather only by a larger accumulation of H_2 (P_{H2} up to 1.43 atm). In addition, the colour of the medium turned completely black and small particles were detected which caused clogging problems in the tube circuit. Again, the electrical supply was cut off and, remarkably, HA production restarted, reaching the fastest production rate (36.64 g m^{-2} d^{-1}) of the whole study, while the H_2 content decreased lowering the total gas pressure (from 1.8 to 1.3 atm). This indicated that at 5 A m^{-2}, biomass might have been inhibited but remained in a latent state, being able to resume metabolism to gas fermentation when conditions turned favourable. The energy per acetate ratio (E:HA) turned out to be maximised at 1.3 A m^{-2} (Table 2), and it was close to the value obtained working under an interrupted power supply. These results are in line with the proposal to operate such systems intermittently by following the fluctuations of renewable energy to produce H_2 when there is excess electricity and convert it into HA when there are no natural resources to generate it.

Table 2
Fixed current supply (A m^{-2}), acetate (HA) production rate (g m^{-2} d^{-1}), energy (E) consumption (Wh d^{-1}) and energy per acetate ratio (E:HA) in kWh kg^{-1} over different current densities and reactors set-ups. HT: H-type cells used in previous thermophilic tests; with continuous (Rovira-Alsina et al., 2020) and intermittent (Rovira-Alsina et al., 2021) electric supply.

Current densityI (A m^{-2})	Acetate productionHA (g m^{-2} d^{-1})	Energy consumptionE (Wh d^{-1})	Energy per Acetate ratioE:HA (kWh kg^{-1})
0.5	0.24	0.57	59.03
1	1.23	1.74	35.54
1.3	5.59	2.23	9.97
1.5	4.25	2.80	16.49
5	0.00	17.41	–
3 (HT)	28.10	8.74	24.00
10 (HT On-Off)	43.27	0.94	7.25

3.3. CO_2 reduction to acetate at bench-scale

With the ultimate goal of operating the ECell at 50 °C with real off-gas feed and interrupted power supply, it was first operated in the

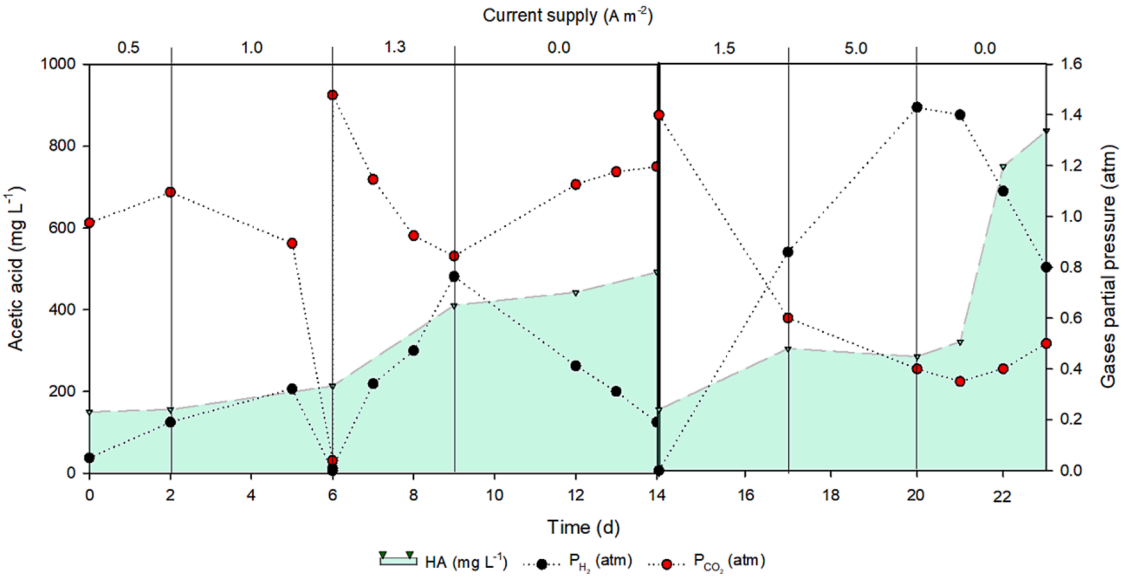

Fig. 2. Acetate (HA) accumulation (mg L^{-1}) and gas partial pressures (atm) of H_2 and CO_2 over time in the ECell at different current densities. The vertical black line indicates two batch-periods.

bench-scale set-up under controlled conditions. This assumed a minimum pH of 4.5, a synthetic CO_2 dissolved content between 750 and 850 mg L^{-1}, a total pressure below 2 atm, and a continuous power supply of 1.3 A m^{-2} (Fig. 3).

During an experimental period of 40 days, HA was produced at a rate of 5.07 g m^{-2} d^{-1}, with a maximum production peak of 24.18 g m^{-2} d^{-1} (between days 12 and 15). The produced H_2 was probably consumed, as the average concentration in the liquid remained low (0.21 ± 0.10 mg L^{-1}), although this could be due to the frequent supply of CO_2, which displaced part of the H_2. CO_2 was added and consumed cyclically, exceeding the lower limit of the marked threshold every approximately half day, while pH profiles had a longer cycle, requiring the addition of base (NaOH 5 M) every 2–3 days. Setting a current density at 1.3 A m^{-2}, resulted in low cumulative energy consumption (0.06 kWh d^{-1}), internal resistance (0.1 Ω cm^{-2}), and cell voltage (between 1.7 V), which translated into a low E:HA ratio (7.39 kWh kg^{-1} HA) if the whole trial is taken into account, and the lowest ratio obtained so far when focusing only on the peak production period (2.07 kWh kg^{-1} HA). Although the energy required for powering the pumps is not considered, this value is lower than the observed for HA formation both, by working with the HT configuration at intermittent energy supply (Table 2) and by commercial methanol carbonylation, which requires 3.53 kWh kg^{-1} HA (Althaus et al., 2007). When compared to other bioelectrosynthesis studies under mesophilic conditions, the difference can be up to 2 orders of magnitude (Arends et al., 2017; Jourdin et al., 2018; Sciarria et al., 2018). On the other hand, CO_2 was consumed at a rate of 182 ± 17 mg L^{-1} d^{-1} during the period of maximum production, while the average for the whole trial decreased to 130 ± 40 mg L^{-1} d^{-1}. Considering also the mean production rate, this implies a CO_2 to HA ratio of 2.21 kg CO_2 kg HA^{-1}. Stoichiometrically, 1.47 kg of CO_2 are needed for the generation of one kg of HA, meaning that part of this CO_2 was also used for microbial growth and maintenance.

Theoretically, if considering the stoichiometric H_2 needed to reach the maximum HA production obtained in previous studies (28 g m^{-2} d^{-1}) with the HT configuration (Rovira-Alsina et al., 2020), a fixed current of 7.5 A m^{-2} would be required working under continuous power supply, while this value would decrease to 2.5 A m^{-2} if intermittent power supply (Rovira-Alsina et al., 2021) could be applied. Therefore, the configuration of the ECell in the bench-scale system resulted in a very good performance in terms of energy utilisation and control of operational variables, as the production rate obtained was the maximum according to stoichiometry, using less energy than with other set-ups. However, 24 g m^{-2} d^{-1} is still far below the value (4100 g m^{-2} d^{-1}) set for industrial commercialisation (Gadkari et al., 2022). Considering that low amounts of H_2 were detected, the system should operate with a higher current supply, but this seemed to be limited by the decomposition of the material due to the combined effect of temperature and electron flow. For MES to work efficiently, the right materials and the right amount of input addition (both current and CO_2 supply) have to be found.

3.4. Considerations to be addressed for scaling up the technology

The bench-scale system proved to be sensitive in its response to the output signals, keeping the operating set points at the desired value or fluctuating the working range when necessary for intelligent management of the processing data. However, the synergy between cause-effect response is as important as the quality of the base components for the scale-up of the technology. In this respect, the reactor material and its layout are key factors to be taken into account.

3.4.1. Electrode material

Even though the ECell was found to be a good electrolyser for H_2 production and the composition of the electrodes was supposed to be pure graphite, the relatively high temperature and current densities seemed to cause a release of substances that could affect the viability of the biomass and hamper the yield. For this reason, a quick quantitative test was conducted with only the electrodes in the synthetic medium to determine the impact that working under these conditions could have on the overall performance (see supplementary material).

The values of OD, pH, EC and sulphur content with the graphite plates in the medium were in the usual range for synthetic media. When the temperature (50 °C) was applied, all variables increased slightly, while the colour of the solution turned green. When a current of 1.3 A m^{-2} was applied, a physicochemical perturbation occurred, which increased OD, EC and sulphur more than 18, 2 and 4 times respectively, compared to the initial values, whereas the colour of the solution changed to a dark black. This indicates that in addition to the temperature, the flow of electrons between the electrodes modifies their state, causing them to deteriorate. Apart from sulphur that can be very toxic to microorganisms, these graphite plates may contain other impurities that can affect the microbial community. Hence, a compromise had to be

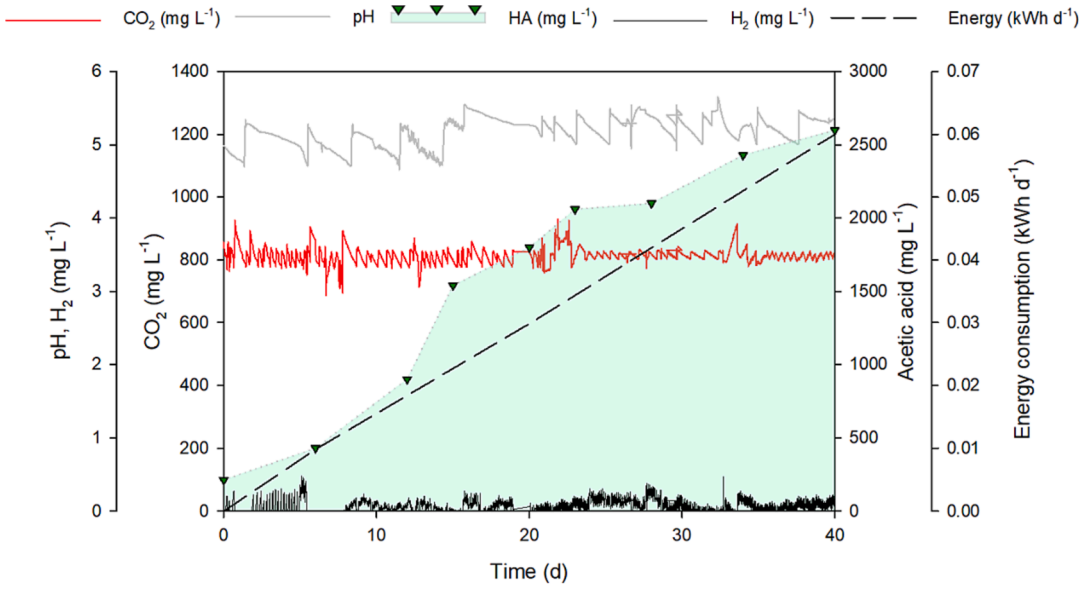

Fig. 3. Acetate (HA) accumulation (mg L^{-1}), pH, H_2 and CO_2 concentration (mg L^{-1}) and power consumption (kWh d^{-1}) over time in ECell reactors using the bench-scale configuration. pH range was controlled between 4.5 and 5.5, CO_2 concentration between 750 and 850 mg L^{-1}, and the total pressure could not exceed 2.1 atm.

found between low current densities and energy-efficient HA production for this particular case.

Graphite is suitable for use as an electrochemical electrode, as it has good electrical conductivity properties, is biocompatible, and the material is still abundant and relatively cheap (Kamal et al., 2020). However, under these operating conditions, it turned out not to be the best choice. Therefore, other materials such as carbon cloth or carbon felt that have proven to be efficient for MES (Zhang et al., 2013) even at high temperatures (Yu et al., 2017), should be tested in the bench-scale configuration.

3.4.2. Internal resistances

The selection of the electrode material is an essential part of the performance of MES. The anode material governs the electrochemical oxidation of the substrates and the subsequent electron transfer to the cathode. Similarly, a good cathode material should reduce the cell potential and enhance the H_2 evolution reaction (Park et al., 2022). However, the distribution of internal resistances in most microbial electrolysis cells remains unclear, making it difficult to optimise and scale up the technology. Varying electrode spacing, inducing fluid movement between electrodes and adjusting the electrode surface area ratio are some strategies that can balance the internal resistance distribution (Miller et al., 2019).

Different reactor configurations with various electrode materials were tested in the bench-scale set-up. The FP reactor using carbon cloth in contact with a graphite rod working as a cathode resulted in feasible operation at higher current densities (5 A m^{-2}) (Fig. 4). However, the decomposition of the anodic graphite increased the internal resistance of the system (from 0.6 to 4.8 Ω cm^{-2}), exceeding the threshold value of the cell voltage (5 V) and cutting off the electric circuit. Although the bio-viability of the system was not compromised, the stability was affected. If a stainless steel wire had been used instead of the graphite rod, the stability would probably have been improved (Blasco-Gómez et al., 2021) but neither HA production (11.28 g m^{-2} d^{-1}) nor the relative production to energy consumption (36.87 kWh kg^{-1}) seemed to be enhanced compared to the ECell set-up.

These results proved that although the purchased reactor design is suitable for scaling up, more configurations, materials and operating conditions still need to be tested to find a proper bioreactor that promotes microbe-material interactions and good gas–liquid mass transfer for efficient HA production. Despite advances in electrode materials research, modifications and cheaper novel alternatives are needed to improve MES performance and overcome the challenges for practical purposes. The design and operation of the bench-scale system were successful in terms of response sensitivity and operational variability. Yet, the results call for intensive investigation of a biocompatible reactor design capable of supplying reducing energy *in situ* without compromising the long-term durability of the biocatalyst. In particular, it is essential to test the MES designs developed on a pilot scale under digitalised control of variables, with an intermittent power supply to increase the product/energy ratio and to apply real off-gases to bring the technology closer to real application.

3.4.3. Outlook

The defined control system consisted of a process variable basis divided into indicator devices giving informative signals (e.g. inlet flow rate, outlet H_2 and O_2 content, conductivity of the medium), or control signals (e.g. inlet pH and CO_2, temperature, pressure) which, depending on the set range, acted on control devices (e.g. acid/base dosing pumps, CO_2 supply, temperature controller flow, overpressure valves). This made it possible to work on different combinations of parameters to increase the selectivity towards HA and to continuously record the response signals immediately after any change, without the need to delay further adjustments.

Temperature had a major influence on both the materials and the biochemical rates. Working at 50 °C increased the average kinetic energy of the reactive molecules, decreasing the internal resistances and boosting the diffusion rate. This could assist the energy input for the endothermic reaction of H_2 production in the cathode, resulting in a lower voltage input (Fu, 2013). However, the limiting factors when working under thermophilic conditions were related to the decreased solubility of gases, the restricted temperature range for most commercial probes, and the underexplored knowledge of thermophilic exoelectrogens. The energy required for heating the bioreactors was also a concern, though the technology could use high-temperature industrial off-gases on-site with a minimum or without further energy addition.

However, even if the selectivity and energy targets could be met, the main limitation to achieving sufficiently high production rates for its scalability will be difficult to overcome. Despite the availability of nutrients, absence of inhibitors, adequate physico-chemical parameters and mixing, the exponential growth and production rates that electrotrophs can achieve are lower than that of heterotrophs, and the values of heterotrophs cannot be compared to those of chemical catalysts. In this sense, instead of envisaging the MES as an industrial process for the massive generation of products, the potential for reducing the carbon footprint and storing renewable energy, albeit in chemical form, could be promoted.

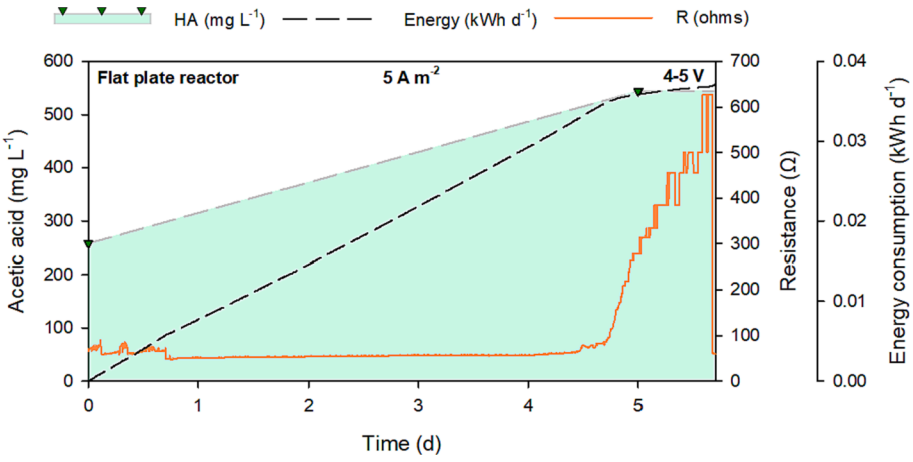

Fig. 4. Acetate (HA) accumulation (mg L^{-1}), ohmic resistance (Ω) and power consumption (kWh d^{-1}) over time in the flat plate reactor with a fixed current supply of 5 A m^{-2}.

4. Conclusions

Real exhaust gases did not hamper the productivity of an open culture, which was able to operate in the long term with similar performance despite the low CO_2 (14%) and high O_2 (12%) content. The optimised design for process control led to an efficient thermophilic CO_2 reduction to HA, obtaining the best compromise between energy and product (2.07 kWh kg^{-1} HA). The limiting H_2 content suggested that higher electric current should be applied to obtain more competitive production rates. However, this requires a combined approach considering biological, electrochemical and economic aspects, keeping the goal of reducing significant amounts of CO_2.

CRediT authorship contribution statement

Laura Rovira-Alsina: Conceptualization, Data curation, Investigation, Methodology, Writing – original draft. **M. Dolors Balaguer:** Conceptualization, Methodology, Supervision, Writing – review & editing. **Sebastià Puig:** Conceptualization, Methodology, Supervision, Funding acquisition, Writing – review & editing.

Declaration of Competing Interest

The authors declare that they have no known competing financial interests or personal relationships that could have appeared to influence the work reported in this paper.

Data availability

Data will be made available on request.

Acknowledgements

This work was supported by the European Union's Horizon 2020 research and innovation program under the grant agreement No 760431 (BioRECO2VER) and the Spanish Ministry of Science and Innovation (PLEC2021-007802 and PID2021-126240OB-I00). LEQUIA (http://www. lequia.udg.edu/) has been recognized as a consolidated research group by the Catalan Government (2017-SGR-1552). L.R.-A. acknowledge the support by the Catalan Government (2018 FI-B 00347) in the European FSE program (CCI 2014ES05SFOP007). S.P is a Serra Hunter Fellow (UdG-AG-575) and acknowledges the funding from the ICREA Academia award.

Appendix A. Supplementary data

Supplementary data to this article can be found online at https://doi.org/10.1016/j.biortech.2022.128161.

References

Althaus H.-J., Chudacoff M., Hischier R., Jungbluth N., Osses M. and Primas A. (2007) Life Cycle Inventories of Chemicals. ecoinvent report No. 8, v2.0. EMPA Dübendorf, Swiss Centre for Life Cycle Inventories, Dübendorf, CH, from www.ecoinvent.org.

Angenent, L.T., Richter, H., Buckel, W., Spirito, C.M., Steinbusch, K.J.J., Plugge, C.M., Strik, D.P.B.T.B., Grootscholten, T.I.M., Buisman, C.J.N., Hamelers, H.V.M., 2016. Chain elongation with reactor microbiomes: open-culture biotechnology to produce biochemicals. Environ. Sci. Technol. 50, 2796–2810. https://doi.org/10.1021/acs.est.5b04847.

Arends, J.B.A., Patil, S.A., Roume, H., Rabaey, K., 2017. Continuous long-term electricity-driven bioproduction of carboxylates and isopropanol from CO2 with a mixed microbial community. J. CO2 Util. 20, 141–149. https://doi.org/10.1016/j.jcou.2017.04.014.

Bajracharya, S., 2016. Microbial Electrosynthesis of Biochemicals. Wageningen University. 10.18174/385426.

Batlle-Vilanova, P., Ganigué, R., Ramió-Pujol, S., Bañeras, L., Jiménez, G., Hidalgo, M., Balaguer, M.D., Colprim, J., Puig, S., 2017. Microbial electrosynthesis of butyrate from carbon dioxide: Production and extraction. Bioelectrochemistry 117, 57–64. https://doi.org/10.1016/j.bioelechem.2017.06.004.

Bian, B., Bajracharya, S., Xu, J., Pant, D., Saikaly, P.E., 2020. Microbial electrosynthesis from CO2: Challenges, opportunities and perspectives in the context of circular bioeconomy. Bioresour. Technol. 302, 122863 https://doi.org/10.1016/j.biortech.2020.122863.

Blasco-Gómez, R., Romans-casas, M., Bolognesi, S., Perona-vico, E., Colprim, J., Balaguer, M.D., Puig, S., 2021. Steering bio-electro recycling of carbon dioxide towards target compounds through novel inoculation and feeding strategies. J. Environ. Chem. Eng. 9, 105549 https://doi.org/10.1016/j.jece.2021.105549.

Christodoulou, X., Okoroafor, T., Parry, S., Velasquez-Orta, S.B., 2017. The use of carbon dioxide in microbial electrosynthesis: Advancements, sustainability and economic feasibility. J. CO2 Util. 18, 390–399. https://doi.org/10.1016/j.jcou.2017.01.027.

Dessì, P., Rovira-Alsina, L., Sánchez, C., Dinesh, G.K., Tong, W., Chatterjee, P., Tedesco, M., Farràs, P., Hamelers, H.M.V., Puig, S., 2020. Microbial electrosynthesis: Towards sustainable biorefineries for production of green chemicals from CO2 emissions. Biotechnol. Adv. 107675 https://doi.org/10.1016/j.biotechadv.2020.107675.

Fruehauf, H.M., Enzmann, F., Harnisch, F., Ulber, R., Holtmann, D., 2020. Microbial Electrosynthesis – An Inventory on Technology Readiness Level and Performance of Different Process Variants. Biotechnol. J. 2000066, 2000066. https://doi.org/10.1002/biot.202000066.

Fu, Q., 2013. A Study on Thermophilic Bioelectrochemical Systems for CO2–to–Methane Conversion Technology.

Gadkari, S., Beigi, H.M., B., Aryal, N., Sadhukhan, J.,, 2022. Microbial electrosynthesis : is it sustainable for bioproduction of acetic acid ? RSC Adv. 9921–9932 https://doi.org/10.1039/d1ra00920f.

Jadhav, D.A., Chendake, A.D., Schievano, A., Pant, D., 2018. Suppressing methanogens and enriching electrogens in bioelectrochemical systems. Bioresour. Technol. https://doi.org/10.1016/j.biortech.2018.12.098.

Jourdin, L., Raes, S.M.T., Buisman, C.J.N., Strik, D.P.B.T.B., 2018. Critical biofilm growth throughout unmodified carbon felts allows continuous bioelectrochemical chain elongation from CO2 up to caproate at high current density. Front. Energy Res. 6 https://doi.org/10.3389/fenrg.2018.00007.

Jourdin, L., Sousa, J., van Stralen, N., Strik, D.P.B.T.B., 2020. Techno-economic assessment of microbial electrosynthesis from CO2 and/or organics: An interdisciplinary roadmap towards future research and application. Appl. Energy 279. https://doi.org/10.1016/j.apenergy.2020.115775.

Kamal, A.S., Othman, R., Jabarullah, N.H., 2020. Preparation and synthesis of synthetic graphite from biomass waste: A review. Syst. Rev. Pharm. 11, 881–894.

Mateos, R., Sotres, A., Alonso, R.M., Morán, A., Escapa, A., 2019. Enhanced CO2 Conversion to Acetate through Microbial Electrosynthesis (MES) by Continuous Headspace Gas Recirculation. Energies. 12 (17), 3297. https://doi.org/10.3390/en12173297.

Miller, A., Singh, L., Wang, L., Liu, H., 2019. Linking internal resistance with design and operation decisions in microbial electrolysis cells. Environ. Int. 126, 611–618. https://doi.org/10.1016/j.envint.2019.02.056.

Molenaar, S.D., Saha, P., Mol, A.R., Sleutels, T.H.J.A., ter Heijne, A., Buisman, C.J.N., 2017. Competition between methanogens and acetogens in biocathodes: A comparison between potentiostatic and galvanostatic control. Int. J. Mol. Sci. 18 https://doi.org/10.3390/ijms18010204.

Park, S.G., Rajesh, P.P., Sim, Y.U., Jadhav, D.A., Noori, M.T., Kim, D.H., Al-Qaradawi, S.Y., Yang, E., Jang, J.K., Chae, K.J., 2022. Addressing scale-up challenges and enhancement in performance of hydrogen-producing microbial electrolysis cell through electrode modifications. Energy Reports 8, 2726–2746. https://doi.org/10.1016/j.egyr.2022.01.198.

Patil, S.A., Gildemyn, S., Pant, D., Zengler, K., Logan, B.E., Rabaey, K., 2015. A logical data representation framework for electricity-driven bioproduction processes. Biotechnol. Adv. 33, 736–744. https://doi.org/10.1016/j.biotechadv.2015.03.002.

Pepè Sciarria, T., Batlle-Vilanova, P., Colombo, B., Scaglia, B., Balaguer, M.D., Colprim, J., Puig, S., Adani, F., 2018. Bio-electrorecycling of carbon dioxide into bioplastics. Green Chem. 20, 4058–4066. https://doi.org/10.1039/c8gc01771a.

Rabaey, K., Rozendal, R.A., 2010. Microbial electrosynthesis - Revisiting the electrical route for microbial production. Nat. Rev. Microbiol. 8, 706–716. https://doi.org/10.1038/nrmicro2422.

Romans-Casas, M., Blasco-Gómez, R., Colprim, J., Balaguer, M.D., Puig, S., 2021. Bio-electro CO2 recycling platform based on two separated steps. J. Environ. Chem. Eng. 9, 105909 https://doi.org/10.1016/j.jece.2021.105909.

Rovira-Alsina, L., Perona-Vico, E., Bañeras, L., Colprim, J., Balaguer, M.D., Puig, S., 2020. Thermophilic bio-electro CO2 recycling into organic compounds. Green Chem. 22, 2947–2955. https://doi.org/10.1039/d0gc00320d.

Rovira-Alsina, L., Balaguer, M.D., Puig, S., 2021. Thermophilic bio-electro carbon dioxide recycling harnessing renewable energy surplus. Bioresour. Technol. 321 https://doi.org/10.1016/j.biortech.2020.124423.

Rovira-Alsina, L., Romans-Casas, M., Balaguer, M.D., Puig, S., 2022. Thermodynamic approach to foresee experimental CO2 reduction to organic compounds. Bioresour. Technol. 354 https://doi.org/10.1016/j.biortech.2022.127181.

Roy, M., Yadav, R., Chiranjeevi, P., Patil, S.A., 2021. Direct utilization of industrial carbon dioxide with low impurities for acetate production via microbial electrosynthesis. Bioresour. Technol. 320, 124289 https://doi.org/10.1016/j.biortech.2020.124289.

Schuchmann, K., Müller, V., 2014. Autotrophy at the thermodynamic limit of life: A model for energy conservation in acetogenic bacteria. Nat. Rev. Microbiol. 12, 809–821. https://doi.org/10.1038/nrmicro3365.

Solomon, S., Plattner, G.K., Knutti, R., Friedlingstein, P., 2009. Irreversible climate change due to carbon dioxide emissions. Proc. Natl. Acad. Sci. U. S. A. 106, 1704–1709. https://doi.org/10.1073/pnas.0812721106.

Song, H., Choi, O., Pandey, A., Kim, Y.G., Joo, J.S., Sang, B.I., 2019. Simultaneous production of methane and acetate by thermophilic mixed culture from carbon dioxide in bioelectrochemical system. Bioresour. Technol. 281, 474–479. https://doi.org/10.1016/j.biortech.2019.02.115.

Su, L., Ajo-Franklin, C.M., 2019. Reaching full potential: bioelectrochemical systems for storing renewable energy in chemical bonds. Curr. Opin. Biotechnol. 57, 66–72. https://doi.org/10.1016/j.copbio.2019.01.018.

Tanner, R.S., Miller, L.M., Yang, D., 1993. Clostridium ljungdahlii sp. nov., an acetogenic species in clostridial rRNA homology group I. Int. J. Syst. Bacteriol. 43, 232–236. https://doi.org/10.1099/00207713-43-2-232.

Van Eerten-jansen, M.C.A.A., Heijne, A.T., Buisman, C.J.N., Hamelers, H.V.M., 2012. Microbial electrolysis cells for production of methane from CO2: long-term performance and perspectives. Int. J. energy Res. 809–819 https://doi.org/10.1002/er.

Vassilev, I., 2019. Microbial electrosynthesis: Anode-and cathode-driven bioproduction of chemicals and biofuels. 10.14264/uql.2019.39.

Verbeeck, K., 2014. Combined Synthesis and Extraction of Acetate From Co 2 Using Microbial Electrosynthesis. Gent.

Virdis, B., Hoelzle, R., Marchetti, A., Boto, S.T., Rosenbaum, M.A., Blasco-Gómez, R., Puig, S., Freguia, S., Villano, M., 2022. Electro-fermentation: Sustainable bioproductions steered by electricity. Biotechnol. Adv. 59, 107950 https://doi.org/10.1016/j.biotechadv.2022.107950.

Von Stockar, U., Maskow, T., Liu, J., Marison, I.W., Patiño, R., 2006. Thermodynamics of microbial growth and metabolism: An analysis of the current situation. J. Biotechnol. 121, 517–533. https://doi.org/10.1016/j.jbiotec.2005.08.012.

Yang, H.Y., Hou, N.N., Wang, Y.X., Liu, J., He, C.S., Wang, Y.R., Li, W.H., Mu, Y., 2021. Mixed-culture biocathodes for acetate production from CO2 reduction in the microbial electrosynthesis: Impact of temperature. Sci. Total Environ. 790, 148128 https://doi.org/10.1016/j.scitotenv.2021.148128.

Yu, L., Yuan, Y., Tang, J., Zhou, S., 2017. Thermophilic Moorella thermoautotrophica-immobilized cathode enhanced microbial electrosynthesis of acetate and formate from CO2. Bioelectrochemistry 117, 23–28. https://doi.org/10.1016/j.bioelechem.2017.05.001.

Zhang, T., Nie, H., Bain, T.S., Lu, H., Cui, M., Snoeyenbos-West, O.L., Franks, A.E., Nevin, K.P., Russell, T.P., Lovley, D.R., 2013. Improved cathode materials for microbial electrosynthesis. Energy Environ. Sci. 6, 217–224. https://doi.org/10.1039/c2ee23350a.